

## Picosecond Raman Studies of the Fröhlich Interaction in Semiconductor Alloys

J. A. Kash, S. S. Jha,<sup>(a)</sup> and J. C. Tsang

*IBM Thomas J. Watson Research Center, Yorktown Heights, New York 10598*

(Received 15 October 1986)

Picosecond Raman studies on the prototypic alloys  $\text{Al}_x\text{Ga}_{1-x}\text{As}$  and  $\text{In}_x\text{Ga}_{1-x}\text{As}$  show that substantial nonequilibrium phonon effects occur in spite of the breakdown in wave-vector conservation engendered by alloy disorder. Phonon lifetimes, measured to be the same as in pure GaAs, also are unaffected by the disorder. Explicit expressions for the Fröhlich couplings of the two LO phonon modes in  $\text{Al}_x\text{Ga}_{1-x}\text{As}$  are obtained to compare with the generation rates of these phonons measured in our experiments.

PACS numbers: 63.20.Kr, 72.10.Di, 78.30.Fs

We study III-V semiconductor alloys with picosecond Raman scattering to characterize quantitatively the effects of alloying on both the Fröhlich interaction and the lifetimes of LO phonons in these materials. In these polar semiconductors, small-wave-vector longitudinal-optic (LO) phonons are excited by the Fröhlich interaction between charged carriers and the long-range dipole fields of these phonons.<sup>1</sup> This interaction dominates the dynamics of highly excited (hot) carriers, and results in so-called "hot-phonon" effects<sup>2</sup> in bulk binary semiconductors such as GaAs and in heterostructures containing both binary and ternary (i.e., alloy) compounds. In ternary semiconductor alloys like  $\text{Al}_x\text{Ga}_{1-x}\text{As}$ , the random substitution of gallium and aluminum causes substantial disorder-related effects on free carriers and excitons.<sup>3</sup> For LO phonons in  $\text{Al}_x\text{Ga}_{1-x}\text{As}$ , cw Raman measurements have revealed<sup>4,5</sup> a substantial asymmetric broadening of the LO-phonon lines, as well as the existence of two distinct LO phonon modes. The broadening has been interpreted in terms of a finite correlation length for the phonons ( $\sim 10$  nm), which leads to an uncertainty in phonon wave vector. This wave-vector uncertainty is greater than the narrow region of momentum space<sup>6</sup> emphasized by the Fröhlich interaction in pure GaAs, and might lead to a substantial increase in the number of phonon modes excited by relaxing hot carriers. Alternatively, the broadening might suggest a decrease of the phonon lifetime. Either of these effects would substantially reduce hot-phonon effects in alloys and possibly in heterostructure devices. We demonstrate here that neither effect occurs, and show why alloying has only a small effect on hot-electron dynamics.<sup>2</sup> Our results are in striking contrast to the well known fact that alloy-disorder-induced scattering plays a significant role in limiting the mobility of carriers in semiconductor alloy systems.<sup>7</sup> At the same time, our results are especially relevant to recent suggestions that III-V alloys may be very well suited for the observation of ballistic transport in device structures and have substantial advantages with regard to their band structure over pure GaAs.<sup>8</sup> Our results show that alloy-disorder scattering will not adverse-

ly effect the band-structure-related advantages of the alloy systems.

In this paper we use the time-domain pump-probe Raman technique<sup>9,10</sup> to measure directly (1) the efficiency of the nonequilibrium phonon production due to the Fröhlich coupling in  $\text{Al}_x\text{Ga}_{1-x}\text{As}$  and  $\text{In}_x\text{Ga}_{1-x}\text{As}$ , (2) LO-phonon lifetimes in  $\text{Al}_x\text{Ga}_{1-x}\text{As}$  and  $\text{In}_x\text{Ga}_{1-x}\text{As}$  in the presence of alloy scattering, and (3) the relative strengths of the Fröhlich coupling for "AlAs-like" and "GaAs-like" LO phonons in the two-mode  $\text{Al}_x\text{Ga}_{1-x}\text{As}$  system. Surprisingly, the production efficiency of Raman-active LO phonons by hot carriers is virtually unchanged from the binary, showing that the atomic disorder does not greatly increase the number of phonon modes that can be excited during hot-carrier relaxation. In addition, the phonon lifetimes that we measure in the alloys are the same as in GaAs, in spite of the spectral broadening observed in cw Raman experiments. These results imply that the lattice dynamics can be described essentially by a pseudo unit-cell model<sup>11</sup> for the crystal, and that the phonon line is inhomogeneously broadened in the alloys. Finally, the strength of the Fröhlich coupling for each of the LO modes in the two-mode  $\text{Al}_x\text{Ga}_{1-x}\text{As}$  system has been derived theoretically, and good agreement is found with our measurements. We show that, while the total electron-LO-phonon scattering rate is nearly constant, the relative strength of each mode is a strong function of alloy composition. These results provide a detailed picture of hot-LO-phonon generation and decay in semiconductor alloys.

Our measurements are performed by our first generating hot carriers with a short laser pump pulse. These carriers in turn generate nonequilibrium LO phonons which are probed with a weaker, delayed pulse of the same wavelength. We use either 0.7- or 5-ps (FWHM autocorrelation) pulses with photon energies between 1.8 and 2.2 eV, pulse repetition rate of 76 MHz, and pump-induced carrier densities of  $5 \times 10^{16}$  to  $10^{17}$   $\text{cm}^{-3}$ .  $\text{Al}_x\text{Ga}_{1-x}\text{As}$  and GaAs samples were grown by molecular-beam epitaxy or metal-organic chemical-vapor deposition, while the  $\text{In}_x\text{Ga}_{1-x}\text{As}$  samples were grown by

metal-organic molecular-beam epitaxy.<sup>12</sup> Further experimental details are in Ref. 10. The phonon spectra were superimposed on a background of broad-band hot luminescence<sup>13</sup> which was subtracted.

In Fig. 1(a) we show the Raman spectrum observed for a 0.7-ps probe pulse coming 10 ps before the 0.7-ps pump pulse (dashed curve), i.e., no nonequilibrium phonons, and the *additional* scattering induced when the probe follows the pump by 2 ps (solid curve). Figure 1(b) gives the variation of this nonequilibrium phonon population  $\Delta n$  versus probe delay for LO phonons in GaAs and the GaAs-type LO phonon mode in  $\text{Al}_{0.24}\text{Ga}_{0.76}\text{As}$ . There is no substantial difference in either the peak nonequilibrium mode occupancy ( $\Delta n \sim 0.06$ ) or the decay time (about 3.5 ps). Small differences in the observed rise times and peak  $\Delta n$ 's correlate with changes in the band gap (1.42 eV for GaAs, 1.77 eV for  $\text{Al}_{0.24}\text{Ga}_{0.76}\text{As}$ ), similar to changes we have observed in GaAs for different laser photon energies.<sup>14</sup> Similar results are observed in other  $\text{Al}_x\text{Ga}_{1-x}\text{As}$  samples ( $x=0.07$  and 0.17) and in an  $\text{In}_x\text{Ga}_{1-x}\text{As}$  sample ( $x=0.10$ ), which, in contrast to  $\text{Al}_x\text{Ga}_{1-x}\text{As}$ , shows only a single LO pho-

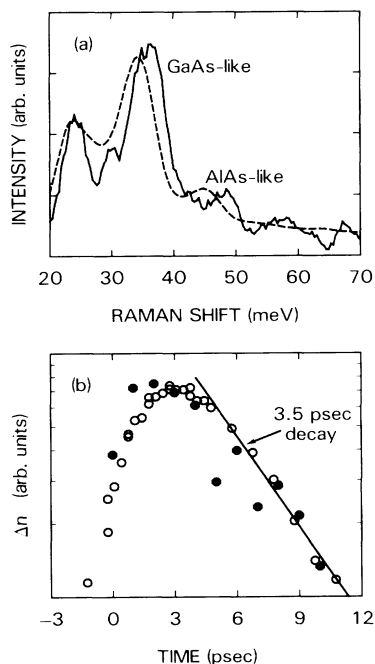


FIG. 1. (a) Raman scattering excited in room-temperature  $\text{Al}_{0.24}\text{Ga}_{0.76}\text{As}$  for 0.7-ps pulses at 2.19 eV. The dashed curve is for the probe preceding the pump by 10 ps, and the solid curve is the additional scattering ( $\times 10$ ) when the probe follows the pump by 2 ps. The small shift between the curves for the GaAs-type mode is due to a slight coupling to the plasmon mode at the injected carrier density of about  $10^{17} \text{ cm}^{-3}$ . (b) Nonequilibrium phonon kinetics vs time for GaAs (open circles) and  $\text{Al}_{0.24}\text{Ga}_{0.76}\text{As}$  (filled circles). Laser photon energy for the GaAs data was 2.13 eV.

TABLE I. Measured LO and TO phonon frequencies and (in parentheses) FWHM linewidths. For the AlAs-type TO phonon, the frequency  $\omega_{1t}$  is calculated as explained in the text.

	$\omega_{2l}$ (GaAs type) ( $\text{cm}^{-1}$ )	$\omega_{2t}$ (GaAs type) ( $\text{cm}^{-1}$ )	$\omega_{1l}$ (AlAs type) ( $\text{cm}^{-1}$ )	$\omega_{1t}$ (AlAs type) ( $\text{cm}^{-1}$ )
GaAs	292 (2.6)	268	...	...
$\text{Al}_{0.07}\text{Ga}_{0.93}\text{As}$	290 (3.7)	268	362 (7.1)	360
$\text{Al}_{0.17}\text{Ga}_{0.83}\text{As}$	285 (3.7)	265	370 (12.4)	365
$\text{Al}_{0.24}\text{Ga}_{0.76}\text{As}$	282 (3.7)	265	374 (10.2)	366

non mode. To characterize the phonon frequencies and linewidths for our samples we separately measured cw Raman spectra. These results are reported in Table I. The phonon lines are asymmetrically broadened to lower energies for the alloy samples.<sup>4,5</sup> Since we are unable to resolve the peak of the AlAs-type TO phonon ( $\omega_{1t}$ ), we have used the generalized Lyddane-Sachs-Teller relation [see Eq. (2)] to obtain the value of  $\omega_{1t}$  from the other measured phonon frequencies of our samples. Values for  $\epsilon_0$  and  $\epsilon_\infty$  as functions of  $x$  are linearly interpolated from pure GaAs ( $\epsilon_0=12.8$ ,  $\epsilon_\infty=10.9$ ) and pure AlAs ( $\epsilon_0=12.0$ ,  $\epsilon_\infty=9.6$ ).<sup>15</sup>

Because of the broad spectral width of the subpicosecond laser and the relatively weak scattering of the AlAs-type LO mode in  $\text{Al}_x\text{Ga}_{1-x}\text{As}$ , we used 5-ps pulses to study the nonequilibrium AlAs-type LO phonons. From the results (Fig. 2), we deduce that the rise time and decay time of the AlAs-type mode are the same

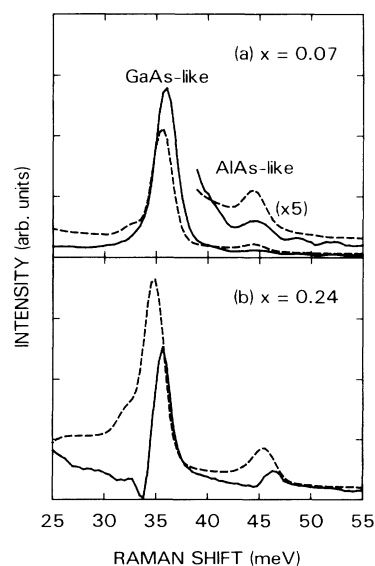


FIG. 2. Raman scattering from  $\text{Al}_x\text{Ga}_{1-x}\text{As}$  as in Fig. 1(a), except that laser pulses are 5 ps long. The nonequilibrium phonons (solid curves) are scaled  $\times 5$  compared to the background thermal phonons (dashed curves).

as the GaAs-type mode to within 25%. Because the kinetics of both modes are quite similar, we can use Fig. 2 to deduce the relative efficiency of phonon production due to the Fröhlich coupling for each of the two modes. We do this by comparing the ratio of the nonequilibrium population of a given mode to the known thermal population for the same mode (i.e.,  $\Delta n$  is the room-temperature thermal occupation times the ratio of difference peak to background peak in Fig. 2). These results (Fig. 3, open circles) show that for small values of  $x$ , the coupling of electrons to the AlAs-type mode is much weaker than the coupling to the GaAs-type mode, and also much smaller than the coupling expected in pure AlAs.

To understand these experimental results, we examine the Fröhlich coupling for a two-mode semiconductor alloy. In the random element isodisplacement model<sup>11,16</sup> or other more realistic models<sup>15,17</sup> which can give the two-mode behavior observed in  $\text{Al}_x\text{Ga}_{1-x}\text{As}$ , for any dependence of the dynamical force matrix on  $x$ , the long-wavelength dielectric function can be written quite generally as

$$\epsilon(\omega) = \epsilon_\infty + S_1 \omega_{1l}^2 (\omega_{1l}^2 - \omega^2)^{-1} + S_2 \omega_{2l}^2 (\omega_{2l}^2 - \omega^2)^{-1},$$

where  $\epsilon_\infty = 1 + 4\pi P_e/E$  arises from the high-frequency electronic polarization and the last two terms come from the ionic polarizations corresponding to the two optical eigenmodes, the AlAs-type mode and GaAs-type mode, respectively. Here,  $\omega_{1l}$  and  $\omega_{2l}$  are the corresponding TO frequencies and  $S_1$  and  $S_2$  are the oscillator

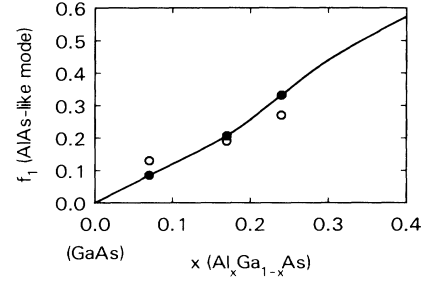


FIG. 3. Fraction  $f_1$  of nonequilibrium phonons which are AlAs type vs alloy composition. Theory (curve and filled circles) are from Eq. (5) as explained in the text.

strengths, all of which depend on  $x$ . The zeros of  $\epsilon(\omega)$  determine the two LO frequencies as functions of  $x$  in the forms

$$\omega_{1l}^2 + \omega_{2l}^2 = \omega_{1t}^2 + \omega_{2t}^2 + (S_1 \omega_{1l}^2 + S_2 \omega_{2l}^2) / \epsilon_\infty, \quad (1)$$

$$\omega_{1l}^2 \omega_{2l}^2 = \omega_{1t}^2 \omega_{2t}^2 (\epsilon_\infty + S_1 + S_2) / \epsilon_\infty = \omega_{1t}^2 \omega_{2t}^2 \epsilon_0 / \epsilon_\infty. \quad (2)$$

The ionic polarization in the crystal is given by

$$P^{\text{ion}} = N[xe_1 u_1 + (1-x)e_2 u_2 + e_3 u_3],$$

where  $N$  is the ion-pair density,  $e_1, e_2$ , and  $e_3$  are ionic charges for Al, Ga, and As ions, with  $e_3 = -xe_1 - (1-x)e_2$  (charge neutrality), and  $u_1, u_2$ , and  $u_3$  are their displacements. In terms of eigen displacement vectors  $v^{(i)}$  obtained after diagonalization of the dynamical matrix,<sup>17</sup> the longitudinal part of the ionic polarization can be rewritten as

$$P_l^{\text{ion}} = N[(S_1 \omega_{1l}^2 / 4\pi N)^{1/2} v_l^{(1)}(\mathbf{r}) + (S_2 \omega_{2l}^2 / 4\pi N)^{1/2} v_l^{(2)}(\mathbf{r})]. \quad (3)$$

The longitudinal electric field associated with the long-wavelength LO oscillations can be obtained from the relation  $E_l = -4\pi P_l^{\text{ion}} - (\epsilon_\infty - 1)E_l = -4\pi P_l^{\text{ion}} / \epsilon_\infty$ , from which the Fröhlich Hamiltonian can be calculated by use of  $H_F = -e\phi_l(\mathbf{r})$ ,  $\mathbf{E}_l = -\nabla\phi_l(\mathbf{r})$  at the electronic coordinate  $\mathbf{r}$ . Note that  $S_1$  and  $S_2$  in Eq. (3) can be eliminated in favor of  $\Delta_1^2 \equiv \omega_{1l}^2 - \omega_{1t}^2$  and  $\Delta_2^2 \equiv \omega_{2l}^2 - \omega_{2t}^2$  by use of Eqs. (1) and (2). On expansion of the eigen displacement vectors in terms of the usual boson creation and annihilation operators for phonons,

$$v_l^{(i)}(\mathbf{r}) = \sum_q (\hbar/2\omega_{il})^{1/2} \hat{e}_{il} [a_{iq} \exp(i\mathbf{q}\cdot\mathbf{r}) + a_{iq}^\dagger \exp(-i\mathbf{q}\cdot\mathbf{r})],$$

the final expression for the Fröhlich Hamiltonian is

$$H_F = \left[ \frac{4\pi N e^2}{\epsilon_\infty} \right]^{1/2} \sum_q \frac{i}{q} \left[ \Delta_1 \left( 1 + \frac{\Delta_2^2}{(\omega_{2l}^2 - \omega_{1t}^2)} \right) \right]^{1/2} \left[ \frac{\hbar}{2\omega_{1l}} \right]^{1/2} (a_{1q} e^{i\mathbf{q}\cdot\mathbf{r}} - a_{1q}^\dagger e^{-i\mathbf{q}\cdot\mathbf{r}}) \\ + \Delta_2 \left( 1 + \frac{\Delta_1^2}{(\omega_{1l}^2 - \omega_{2t}^2)} \right) \right]^{1/2} \left[ \frac{\hbar}{2\omega_{2l}} \right]^{1/2} (a_{2q} e^{i\mathbf{q}\cdot\mathbf{r}} - a_{2q}^\dagger e^{-i\mathbf{q}\cdot\mathbf{r}}). \quad (4)$$

In our obtaining Eq. (4), the phonon wave functions have been assumed to be plane waves. To introduce the effects of alloy disorder, a finite correlation length for the phonon wave function<sup>5</sup> is more appropriate. In the calculation of the matrix element of  $H_F$ , this will restrict the spatial integral to a finite effective volume. However, the Fröhlich interaction contains the inverse gradient operator arising from  $\mathbf{E}_l = -\nabla\phi_l(\mathbf{r})$ . This implies that the Fröhlich coupling still produces mainly the "long

wavelength" phonons that are observed in Raman scattering. Our lifetime measurements imply that the homogeneous linewidth of the LO phonons remains constant, in spite of the substantial changes seen in these phonon linewidths upon alloying. Consistent with the model of Parayanthal and Pollak,<sup>5</sup> the observed broadening and asymmetry result from an inhomogeneous superposition of modes of different  $q$ .

When we apply the usual Fermi "golden rule," Eq. (4) gives the electron-phonon scattering rate for each of the LO phonon modes in  $\text{Al}_x\text{Ga}_{1-x}\text{As}$ . If we ignore small differences arising from the densities of final states, the fractional AlAs-type mode scattering rate compared to the total electron-phonon scattering rate is approximately given by

$$f_1 \approx \Delta_1^2 [1 - \Delta_2^2 / (\omega_{1t}^2 - \omega_{2t}^2)] / (\Delta_1^2 + \Delta_2^2). \quad (5)$$

Since the TO phonon frequencies vary little with alloy composition,<sup>4</sup> the total coupling strength for both modes depends only slightly on composition. On the other hand, Eq. (5) shows that the coupling to a given mode is a strong function of alloy composition, depending directly on the ionicity  $\Delta_i$  of the mode. Theoretical values for  $f_1$  in our samples are shown in Fig. 3 as solid circles. As inputs, we have used the phonon frequencies from Table I. The smooth curve connecting these points was extended beyond  $x=0.24$  by the same procedure on data reported in Ref. 4. Our experimentally measured values of  $f_1$  for the same samples are shown as open circles. There are no adjustable parameters, and the agreement is remarkably good.

In conclusion, we have found that the Fröhlich contribution to the electron-LO-phonon interaction in both the two-LO-phonon mode system  $\text{Al}_x\text{Ga}_{1-x}\text{As}$  and one-LO-phonon mode system  $\text{In}_x\text{Ga}_{1-x}\text{As}$  is quantitatively similar to its contribution in pure GaAs despite alloying which broadens the phonon lines and can create a two-mode system. The broadening, which has been interpreted in terms of phonons with relatively short correlation lengths as compared to the binary compound, neither reduces the LO phonon lifetime nor significantly decreases the efficiency of the coupling of hot carriers to the small-wave-vector LO phonons, which are the Raman-active LO phonons. Since the observation of hot-phonon effects in GaAs depends on the efficient excitation of relatively long-lived LO phonons with small wave vectors, we have demonstrated that these effects should also be present in alloys of GaAs. We have been able to observe nonequilibrium phonons for both the GaAs-type mode and the AlAs-type mode in our  $\text{Al}_x\text{Ga}_{1-x}\text{As}$  samples. The total coupling to both modes is roughly independent of alloy composition. The strong variation with composition of the relative magnitudes of the nonequilibrium populations for the modes shows

clearly the direct relation between the spectroscopic ionicity of the phonon mode and the strength of the electron-LO-phonon scattering for that mode. These results, when combined with the dominant role of small-wave-vector LO-phonon scattering in determining the hot-electron relaxation rates in these materials, show that the hot-electron relaxation is much less susceptible to alloy scattering than the normal transport properties.

We thank T. Kuech and W. Wang for providing the GaAs and  $\text{Al}_x\text{Ga}_{1-x}\text{As}$  samples, and H. Lüth, N. Pütz, E. Veuhoff, H. Heinecke, M. Heyen, and P. Balk of the Technical University of Aachen for the  $\text{In}_x\text{Ga}_{1-x}\text{As}$  sample.

(a)Permanent address: Tata Institute of Fundamental Research, Bombay 400005, India.

<sup>1</sup>E. M. Conwell and E. O. Vassel, IEEE Trans. Electron. Devices **13**, 22 (1966).

<sup>2</sup>For example, P. Kocevar, Physica (Amsterdam) **134B**, 155 (1985).

<sup>3</sup>For example, E. Cohen and M. D. Sturge, Phys. Rev. B **25**, 3828 (1982).

<sup>4</sup>Bernard Jusserand and Jacques Sapriel, Phys. Rev. B **24**, 7194 (1981).

<sup>5</sup>P. Parayanthal and Fred H. Pollak, Phys. Rev. Lett. **52**, 1822 (1984).

<sup>6</sup>C. L. Collins and P. Y. Yu, Phys. Rev. B **30**, 4501 (1984).

<sup>7</sup>A. Amith, Phys. Rev. **139**, A1624 (1965); A. K. Saxena, Phys. Rev. B **24**, 3295 (1981); A. K. Saxena and A. R. Adams, J. Appl. Phys. **58**, 2640 (1985).

<sup>8</sup>A. F. J. Levi, J. R. Hayes, and R. Bhat, Appl. Phys. Lett. **48**, 1609 (1986).

<sup>9</sup>D. von der Linde, J. Kuhl, and H. Klingenburg, Phys. Rev. Lett. **44**, 1505 (1980).

<sup>10</sup>J. A. Kash, J. C. Tsang, and J. M. Hvam, Phys. Rev. Lett. **54**, 2151 (1985).

<sup>11</sup>I. F. Chang and S. S. Mitra, Adv. Phys. **20**, 359 (1971).

<sup>12</sup>N. Pütz, E. Veuhoff, H. Heinecke, M. Heyen, H. Lüth, and P. Balk, J. Vac. Sci. Technol. B **3**, 671 (1985).

<sup>13</sup>J. C. Tsang and J. A. Kash, Phys. Rev. B **34**, 6003 (1986).

<sup>14</sup>J. A. Kash, unpublished.

<sup>15</sup>R. Bonneville, Phys. Rev. B **24**, 1987 (1981).

<sup>16</sup>E. Ilegems and G. L. Pearson, Phys. Rev. B **1**, 1576 (1970); I. F. Chang and S. S. Mitra, Phys. Rev. B **2**, 1215 (1970).

<sup>17</sup>H. W. Verleur and A. S. Barker, Phys. Rev. **149**, 715 (1966).